Thin Solid Films 531 (2013) 408–414

Contents lists available at SciVerse ScienceDirect

Thin Solid Films

journal homepage: www.elsevier.com/locate/tsf

Electrical and spectral characteristics of an atmospheric pressure argon plasma jet generated with tube-ring electrodes in surface dielectric barrier discharge

Y. Hong [a,b], N. Lu [a], J. Pan [b], J. Li [a,*], Y. Wu [a]

[a] Institute of Electrostatics and Special Power, Dalian University of Technology, Dalian 116024, People's Republic of China
[b] Department of Physics and Electrical Engineering, Weinan Teachers University, Weinan 71400, People's Republic of China

ARTICLE INFO

Article history:
Received 27 February 2012
Received in revised form 21 December 2012
Accepted 7 January 2013
Available online 31 January 2013

Keywords:
Conduction current
Electric-field
Electron temperature
Oxygen atomic density

ABSTRACT

An atmospheric-pressure argon plasma jet is generated with tube-ring electrodes in surface dielectric barrier discharge by a sinusoidal excitation voltage at 8 kHz. The electrical and spectral characteristics are estimated such as conduction and displacement current, electric-field, electron temperature, rotational temperature of N_2 and OH, electronic excitation temperature, and oxygen atomic density. It is found that the electric-field magnitudes in the top area of the ground electrode are higher than that in the bottom area of the power electrode, and the electron temperature along radial direction is in the range of 9.6–10.4 eV and along axial direction in the range of 4.9–10 eV. The rotational temperature of N_2 obtained by comparing the simulated spectrum with the measured spectrum at the $C^3\Pi_u \rightarrow B^3\Pi_g(\Delta v = -2)$ band transition is in the range of 342–387 K, the electronic excitation temperature determined by Boltzmann's plot method is in the range of 3188–3295 K, and the oxygen atomic density estimated by the spectral intensity ratio of atomic oxygen line $\lambda = 844.6$ nm to argon line $\lambda = 750.4$ nm is in the order of magnitude of 10^{16} cm^{-3}, respectively.

1. Introduction

Atmospheric-pressure nonequilibrium plasmas (APNPs) have critical advantages compared with widely used low-pressure plasmas, because they do not require expensive and complicated vacuum systems and can replace the low-pressure plasma devices in some existing applications, such as biomedical and chemical decontamination [1,2], surface modification [3], materials processing [4], thin film deposition [5–7], etching [8], and sterilization [9–12]. Among APNPs, the atmospheric-pressure cold plasma jets have indisputable advantages, which contain a large number of active species and formed in open air, so the short lifetime active species such as oxygen atoms and charge particles can be transported easily to the surfaces of the objects treated before disappearing, and there are no limitations to the sizes of the objects to be treated.

According to the configurations of electrodes in the discharge device, atmospheric-pressure cold plasma jets can be classified for two main types of electrode geometry: 'bare' powered electrodes and dielectric covered electrodes [13]. For example, Huang and Li [14] developed an atmospheric-pressure argon plasma jet, which was generated with a single needle electrode by a sinusoidal alternating-current power supply with an operating frequency of 45 kHz. The plasma jet was employed to perform some applications such as treatment of interior surface of a medical infusion tube, hydrophilic modification of insulator surface, hardening of metal surface, and acidification treatment of water. Laroussia and Lu [15] presented an atmospheric-pressure helium plasma jet generated with two thin copper rings attached to the surface of a centrally perforated glass disk in dielectric barrier discharge (DBD) by submicrosecond high voltage pulsed power with repetition rates in the 1–10 kHz range. The generated plasma plume was several centimeters long and could be touched by the bare hands without causing any heating or painful sensation. Walsh et al. [16] reported room temperature atmospheric argon plasma jet generated with a single ring electrode made of a 1 cm wide metal strip in DBD by submicrosecond voltage pulses at 4 kHz. The pulsed argon plasma jet operated continuously for many hours without rising to any marked temperature and the electron density was 3.9 times greater than that in a comparable sinusoidal jet.

The major advantages of the DBD configuration is to prevent the transition to spark and to homogenize the discharge [13]. Based on this property, a cold atmospheric-pressure argon plasma jet with tube-ring electrodes in surface dielectric barrier discharge (SDBD) is generated by a sinusoidal excitation voltage at 8 kHz. The electrical and spectral characteristics are obtained such as applied voltage, conduction and displacement current, electric-field, electron temperature, rotational temperature of N_2 and OH, electronic excitation temperature, and oxygen atomic density.

2. Experimental setup

A schematic of experimental apparatus and discharge photograph are shown in Fig. 1. The power electrode is a stainless steel tube with an outer diameter of 8 mm, an inner diameter of 6 mm, and a length of

* Corresponding author. Tel./fax: +86 411 84708576.
E-mail address: lijie@dlut.edu.cn (J. Li).

0040-6090/$ – see front matter © 2013 Elsevier B.V. All rights reserved.
http://dx.doi.org/10.1016/j.tsf.2013.01.056

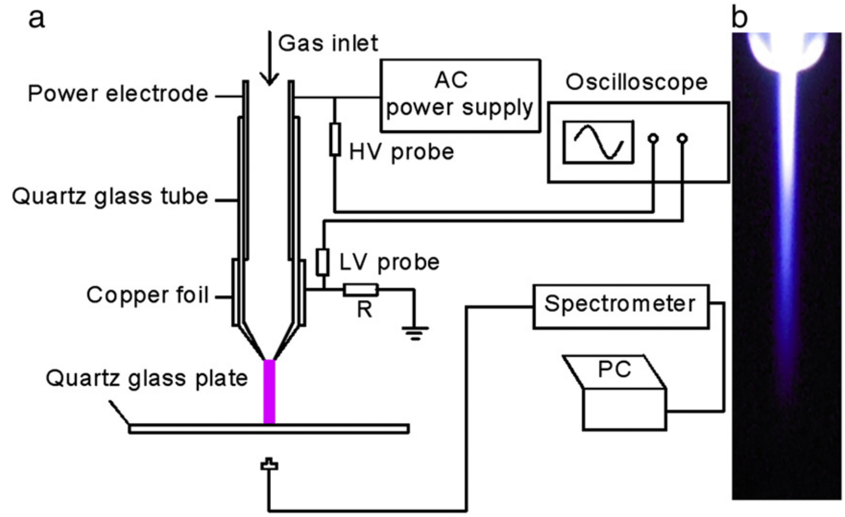

Fig. 1. Experimental setup of the plasma jet device (a) and discharge photograph at a peak applied voltage of 6.2 kV and Ar flow rate of 1 L/min (b).

128 mm. It is powered by a sinusoidal excitation voltage at 8 kHz. The power electrode is attached tightly on the inside wall of a quartz glass tube with an outer diameter of 10 mm, an inner diameter of 8 mm, and a length of 100 mm. The pencil-shaped tapered open end of the quartz glass tube is used as a gas outlet, the diameter of which is 2 mm. The ground electrode is a 20 mm wide copper foil wrapped on the outside of the quartz glass tube, and the top of which is at the same height with the bottom of the power electrode. A quartz glass plate (thickness of 1 mm) is placed in a position of 5 mm away from the gas outlet.

The working gas of Ar (99.999%) is injected through the power electrode controlled by a mass flow controller at a flow rate of 1 L/min. The applied voltages are measured using a high voltage probe (Tektronix P6015A) and the currents are measured through a 50 Ω resistor in series with the ground electrode, and the electrical signals are recorded via a digital oscilloscope (Tektronix TDS 2012B). An optical fiber located in a position of 2 mm away from the quartz glass plate is used to collect the optical emission of the plasma plume, and the signals are recorded by a spectrometer (Acton INS-300-122B) with a grating of 1200 grooves per millimeter and a slit width of 20 μm. The plasma jet lengths and discharge images are obtained by a Nikon digital camera COOLPIX S600.

3. Experiment results and discussions

3.1. Electrical discharge characteristics

In accordance with the schematic of an asymmetric single dielectric barrier plasma actuator reported by Singh et al. [17], we impose a virtual electrode paralleled to the ground electrode over the inside wall of the quartz glass tube. Fig. 2 shows an equivalent circuit diagram of the

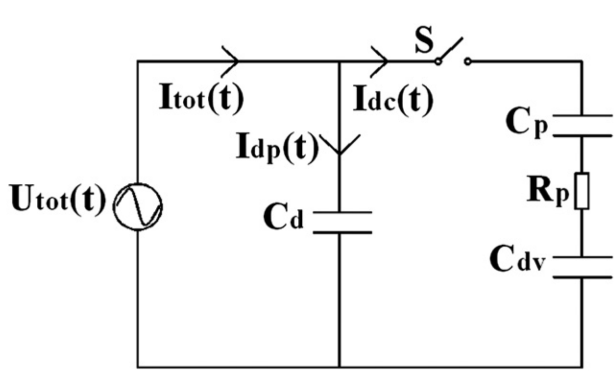

Fig. 2. Equivalent circuit diagram of the plasma jet device.

plasma jet device. As shown in Fig. 2, C_d represents the capacitor between the power electrode and the ground electrode, C_{dv} represents the capacitor between the virtual electrode and the ground electrode, and C_p and R_p represent the equivalent capacitance and the resistance of plasma jet, respectively. Accordingly, the plasma jet device is essentially a capacitor C_p and a resistor R_p in series with a capacitor C_{dv} and a capacitor C_d parallel to the full circuit. Also, $U_{tot}(t)$ represents the externally excited voltage, $I_{tot}(t)$ represents the total current, $I_{dc}(t)$ represents the conduction current through gas gap, and $I_{dp}(t)$ represents the displacement current through dielectric.

Using Kirchoff's theorem for the equivalent circuit given in Fig. 2, the following equations are obtained

$$\frac{dU_{tot}(t)}{dt} = \frac{I_{dp}(t)}{C_d}, \tag{1}$$

$$I_{tot}(t) = I_{dp}(t) + I_{dc}(t). \tag{2}$$

In Eq. (1), C_d is deduced from the data of applied voltage and displacement current. The applied voltage is measured using a high voltage probe (Tektronix P6015A), and displacement current is measured without discharging in the reactor when air replaces the argon as the working gas [18]. Fig. 3(a) shows the waveforms of applied voltage, total current, displacement and conduction current measured at a peak applied voltage of 2 kV. The total current is measured through a 50 Ω resistor in series with the ground electrode, which consists of a displacement and conduction current. Therefore, the conduction current is determined by subtracting the displacement current from the total current. Regarding the results shown in Fig. 3(a), the waveforms of total current and applied voltage have a phase difference of nearly 90°, indicating that the impedance of the reactor is capacitive. The displacement component takes up a large proportion in the total current, and some weak micropeaks on the main current-pulse of conduction current and total current appear at every half-period, which is similar to the typical characteristic of atmospheric-pressure DBD [18]. Fig. 3(b) shows the capacitance waveform of the capacitor C_d for two periods obtained using Eq. (1) with the data in Fig. 3(a). As presented in Fig. 3(b), two peaks appeared symmetrically in every half-period, which arises due to numerical singularities occurring during the zero crossing of the denominator [19,20]. Therefore, the average value of C_d is determined without considering the effect of peaks equal to 3.7 pF.

Fig. 4 shows the waveforms of applied voltage, total current, displacement and conduction current at a peak applied voltage of 6.4 kV. At a peak applied voltage of 6.4 kV the displacement current cannot be measured, because the discharge occurs in the reactor when the air